UNIZIK JOURNAL OF ENGINEERING AND APPLIED SCIENCES (UJEAS)

Research Article

Hysteresis of polyamide 12/ethylene propylene diene monomer polymeric blends filled with nano-clay under cyclic loading: Experimental approach

Friday Nwankwo Archibong, Louis Chukwuemeka Orakwe, Joseph Ikenna Ubah, Victor Chijioke Okafor

Special Issue
A Themed Issue in Honour of Professor Clement Uche Atuanya on His retirement.

This themed issue pays tribute to Professor Clement Uche Atuanya in recognition of his illustrious career in Metallurgical and Materials Engineering as he retires from Nnamdi Azikiwe University, Awka. We celebrate his enduring legacy of dedication to advancing knowledge and his impact on academia and beyond through this collection of writings.

Edited by
Chinonso Hubert Achebe PhD.
Christian Emeka Okafor PhD.

UJEAS

UNIZIK JOURNAL OF ENGINEERING AND APPLIED SCIENCES

UNIZIK Journal of Engineering and Applied Sciences 3(3), September (2024), 995-1004
Journal homepage: https://journals.unizik.edu.ng/index.php/ujeas
PRINT ISSN: 2992-4383 || ONLINE ISSN: 2992-4391

Hysteresis of polyamide 12/ethylene propylene diene monomer polymeric blends filled with nano-clay under cyclic loading: Experimental approach

Friday Nwankwo Archibong[1,2*], Louis Chukwuemeka Orakwe[2], Joseph Ikenna Ubah[2], Victor Chijioke Okafor[3]
[1]Department of Mechanical Engineering, Faculty of Engineering, Alex Ekwueme Federal University Ndufu-Alike Ikwo.
[2]Department of Agricultural &Bioresources Engineering, Faculty of Engineering, Nnamdi Azikiwe University, Awka.
[3]Department of Agricultural & Bioresources Engineering, University of Technology Owerri.
[*]Corresponding Author's E-mail: fridayashibong@gmail.com

Abstract
Polyamide 12 (PA12) is a type of polymer extensively used in many applications due to its strength, low water absorption and density. Blending PA12 with elastomers and other consumer polymers expand its applications. Pure ethylene propylene diene monomer (EPDM) is soft and elastic, which limits it load bearing applications. To overcome such limitation, PA12 and EPDM can be greatly improved by reinforcing the matrix with Cloisite 30B (C30B). The only objective is to determine the Mullins effect of EPDM and C30B when blended with PA12. The three constituents were simultaneously mixed by using an internal mixer (Haake Rheomix 600) at a blade rotational speed of 100 rpm, during 6 or 3 mins, at 200 ºC. To minimize the degradation of the composite components during mixing, especially the alkyl ammonium ions, the processing temperature was fixed at 200 °C, which corresponds to less 20 ^{0}C above the melting point of PA12. All samples were pelletized by compression moulding at 200 °C between 2 mm thick plates, at several C30B mass fractions ranging from 0 to 5 w.t%. Cyclic tension tests are conducted to probe the hysteretic action of the C30B composites. The results show that the stress increased in a separate manner from 10 MPa to 40 MPa. This clearly implies that an increase in the stress response can be realized by increasing the w.t % of either EPDM in the binary composites or C30B in the ternary nanocomposites, meaning that EPDM or C30B can potentially affect the mechanical response. In all the composites, a clear Mullins effect can be noticed as the stress in the reloading operation is lesser than the response of the virgin specimens until striking the beginning of maximum applied strain. Also, a smaller hysteresis loop can be noticed with increase in the amount of C30B into the pure PA12 blend. This work can likely add to understanding the properties of PA12 filled with EPDM and C30B particles and dignify the applications.

Keywords: hysteresis, blends, nano-clay, cyclic loading, stress relaxation, Mullin's effect.

1. Introduction

Nylon came to limelight by Wallace Carothers and first brought to public sale in October 1938 (Sivaram, 2017), and lucratively used for various applications since then. Polyamide-12 (PA12), as one of the types of nylon, has been applied in many different fields, such as consumer goods, electrical and electronics, textile industries, domestic use (Kondo et al., 2022), polyamide 12 nanocomposites applications have created a competitive domain for scientific researchers and industries (Dorigato et al., 2017; Li et al., 2019) and laser sintering systems (Schmid et al., 2017). The mechanical properties of PA12 are pivotal for its usage, which depend on many factors, including mixing temperature, mixing ratios, curing temperature and mixing time (Stojšić et al., 2022; Mahmoud et al., 2024). Ortega et al (2016) observed that curing time and temperature directly affected the linear viscoelastic properties of binary composite of bitumen/montmorillonite. In contrast (Olongal et al., 2021) investigated the effect of MA-g-ABS/ZnO nanoparticles bacteria growth and showed that bacteria colonies is affected by incorporation of ZnO NPs in the composites. Benneghmouche and Benachour (2019) observed that incorporation of nano-clay into the SAN/EPDM increased the

Youngs modulus of the blends. Jeddi et al (2017) observed the dominant role of filler-filler interaction in the viscoelastic behaviour of SAN/EPDM system. Few works like (Krairi & Doghri, 2014; (Salazar et al., 2022; Avanzini et al., 2024) also investigated the viscoelastic and damage behaviours of polyamide 12 and other related polymers.

Much as PA12 has shown promising properties, the modulus of pure PA12 is typically low when compared to binary nanocomposite (Petousis et al., 2022). In addition, the breakage toughness of PA12 is much lower than filled rubbers (Wang et al., 2020; Linul et al., 2020). The low breakage toughness shows that PA12 is brittle meaning that little premature faults can easily grow into huge cracks when subjected to external loading, manifesting to eventual material failure. To overcome this problem, Polyamide 12 composites are blended with nano-clay as reinforcement particles. It has been a long history to use EPDM and nano-clay as fillers to modify the mechanical properties of polymers (Hassan et al., 2015; Baran et al., 2020). It is a known fact that particle size has a major role and strong effect on the mechanical properties of polymer blends. At the onset, there is a consequence of hydrodynamic reinforcement (Meyer et al., 2020; Li et al., 2024). Filler networks may be achieved through weak interparticle bonds with disable polymer (Millereau et al., 2018; Bokobza, 2023).

Many researchers have used cyclic tests to evaluate the mechanical performance of materials. For instance, Wang et al (2015) observed that using cyclic healing can reduce severe plastic deformation and significant shape changes. Another study of (Yin et al., 2024) revealed that the material under study exhibits a different shape to the stress-strain curve upon loading and unloading. It was reported (Schroer & Wheeler, 2018) that deformation under repeated loading is key to further optimize the high-strength of materials. Only few works (Chafidz et al., 2019) have been carried out to probe the performance of polymer composites reinforced with nanoparticles, which obviously showed an enhancement in mechanical properties of the polymer. However, most of these works focused mainly on the monotonic uniaxial tension reactions, while mechanical properties in cyclic loading conditions were not completely explored. To be more precise, the hysteresis conduct of PA12 composites under cyclic loading has not been considered by researchers. It was believed that the hysteresis loop in the stress-strain curves under cyclic loading, which acts for the internal energy debauchery during cycle loading, is firmly connected to the fracture toughness (Long & Hui, 2016; Qi et al., 2018). A huge hysteresis loop shows powerful energy debauchery, and this may remarkably improve the fracture toughness of the material.

Hysteresis in soft material can be caused by two main factors and they are: A – the viscoelastic relaxation outcome. B - the damage-induced stress softening conduct, which is also known as Mullin's effect (Srivastava & Mishra, 2018; Li et al., 2020), this shows that the stress in the reloading process is smaller than the stress response of the neat specimens until the maximum strain in the earlier loading record is reached. Some devices can explain the origin of Mullins effect, such as the damage induced by deformation, the rupture of physically crosslinks (Xiao et al., 2021; Plagge & Klueppel, 2019; Morovati & Dargazany, 2019). On the progress, the Mullins effect outcomes in hysteretic stress-strain links and this is a major mechanism for internal energy debauchery and fracture toughness improvement.

The novelty of this work is centred on the recycling of waste rubber in thermoplastic in an eco-friendly technique. The use of nano-clay as a dispersion agent made this study unique in synergy with thermoplastic and rubber waste. The viscoelasticity of the composites is carried out using cyclic test to determine Mullin's effect. The gap in knowledge include that heavy metals from rubber waste contribute immensely to soil, air and water pollutions (Mohankumar et al., 2016; Banerjee et al., 2019; Gujre et al., 2021). Efforts to reduce it or totally eliminate it gave rise to this study. Fazli & Rodrigue (2020) had a limitation of low affinity and interaction between thermoplastic matrix and crosslinked rubber leading to phase separation and weak adhesion between both phases in their research. The blending of polar polymer and modified clay is difficult to process even though a better properties are obtained as reported by (Mapossa et al., 2023). EPDM has perfect bulk properties according to (Laing et al., 2020), but does not have enough surface energy due to its non-polar character and the movement of low-molecular-weight substances with the surface during mixing and moulding is a drawback (Benneghmouche & Benachour, 2019). The gap to breach the limitation is the use of polar thermoplastic and modified clay to form a ternary composite where EPDM will act as a third component for environmental sustainability.

To the best of our knowledge, no thorough studies on characterization of the hysteresis based on PA12 composites filled with nano-clays under cyclic loading has been published. This work will focus on investigating the Mullins effect on the cyclic loading tests of nano-clay into the PA12 composites. For such purpose, we prepared several binary composites and ternary nanocomposites with PA-12 matrix, elastomer and nanofiller using melt mixing process.

2.0 Material and methods

2.1 Materials

The polymer used as a matrix in this study is a polyamide 12 (PA12), referenced as Rilsan© AECHVO supplied by Indorama Petrochemical Ltd (Portharcourt, Nigeria). The number average molar mass was shown to be 20,000 g/mol and the polydispersity index was found to be 1.9. The melting point of this PA12 grade is 183 ^{0}C. The tensile strength of PA12 is 45 MPa, while density 1.02 gm^{-3}. Elastomer of ethylene propylene diene monomer (EPDM) particles, with an average size of 425 μm and sourced from end-life car door seals, were also used. The silicate dispersed into the matrix is an organically modified montmorillonite clay (OMMT), referenced as Cloisite© 30B (C30B), and supplied by Southern clay products (Gonzales, Texas). C30B is methyl tallow bis-2-hydroxyethyl ammonium exchanged montmorillonite clay with a cationic modifier concentration of 90 milliequivalents per 100 g. The density of this organophilic clay is 1.98 (Aït Hocine et al., 2019).

2.1.1 Preparation of nanocomposites.

Because of the hygroscopic nature of PA-12, it was first dried in a vacuum oven at 80 ˚C for 4 hours prior to mixing. The three constituents were simultaneously mixed by using an internal mixer (Haake Rheomix 600) at a blade rotational speed of 100 rpm, during 6 or 3 mins, at 200 ºC. To minimize the degradation of the composite components during mixing, especially the alkyl ammonium ions, the processing temperature was fixed at 200 ˚C, which corresponds to less 20 ^{0}C above the melting point of PA-12. All samples were pelletized by compression molding at 200 ˚C between 2 mm thick plates, at several C30B mass fractions ranging from 0 to 5 w.t%. The sample code and composition of materials used with their percentage weight are presented in Table 1.

Table 1. The sample code/composition (wt%) of the experimented materials

Sample code	PA12 (%)	EPDM (%)	C30B (%)
PA	100	0	0
PA-E	95	5	0
PA-E	90	10	0
PA-E	80	20	0
PA-E	70	30	0
PA-E-C	89	10	1
PA-E-C	88	10	2
PA-E-C	87	10	3
PA-E-C	85	10	5
PA-C	97	0	3

2.1.1.1 Mechanical tests characterization.

The mechanical properties of the material seen in Table 1 were measured using tension tests. All tests were carried out using MTS criterion model 43 testing machine at a crosshead motion of 0.033 mms^{-1} at 20 °C ambient temperature. The stress relaxation tests were carried out on the unfilled PA12 matrix to probe the viscoelastic behaviours. A 10 MPa force was applied in each 1 s to the specimens and the stress was increased up to 11000 s. Cyclic tension tests were carried out on both unfilled and filled PA12 composites. These cyclic tests were normally used to characterize the Mullins effect on filled rubbers. The cyclic tests play a major role in evaluating the low-frequency mechanical production of elastomer composites for certain applications, for instance, absorbing (damping) materials. The modes used stretched the specimens to the maximum load of 10 MPa and unloaded it to zero force with two cycles, then stretched to 20 MPa and unloaded again in the subsequent cycles. These procedures were repeated until a 50 MPa was reached as shown in Figs. 1 & 2. The tests were operated in two modes, respectively. All samples were subjected to at least 5 cycles and each cycle of the sample specimen is deformed to a stress of 50 MPa and then unloaded to zero force. For uniaxial tension tests, the dumbbell shaped specimens are normally used (Khlystov & Zheng, 2013; Guan et al., 2023; Beerli et al., 2024) as viewed in Fig. 3. Nevertheless, in our elaboration study, it was discovered that fabricating such specimen with such shape is difficult but better than other shapes like the dog bone shape. Seeing that the total applied strain is very small, video extensometer was used to determine the homogeneity of material deformation. It should be noted that the experimental characterization used in this work was carried out using static tests (tests without executing the software code). Therefore, triangular shape of loading is applied (where magnitude is zero at one end of the span and increases constantly till the second end of the span).

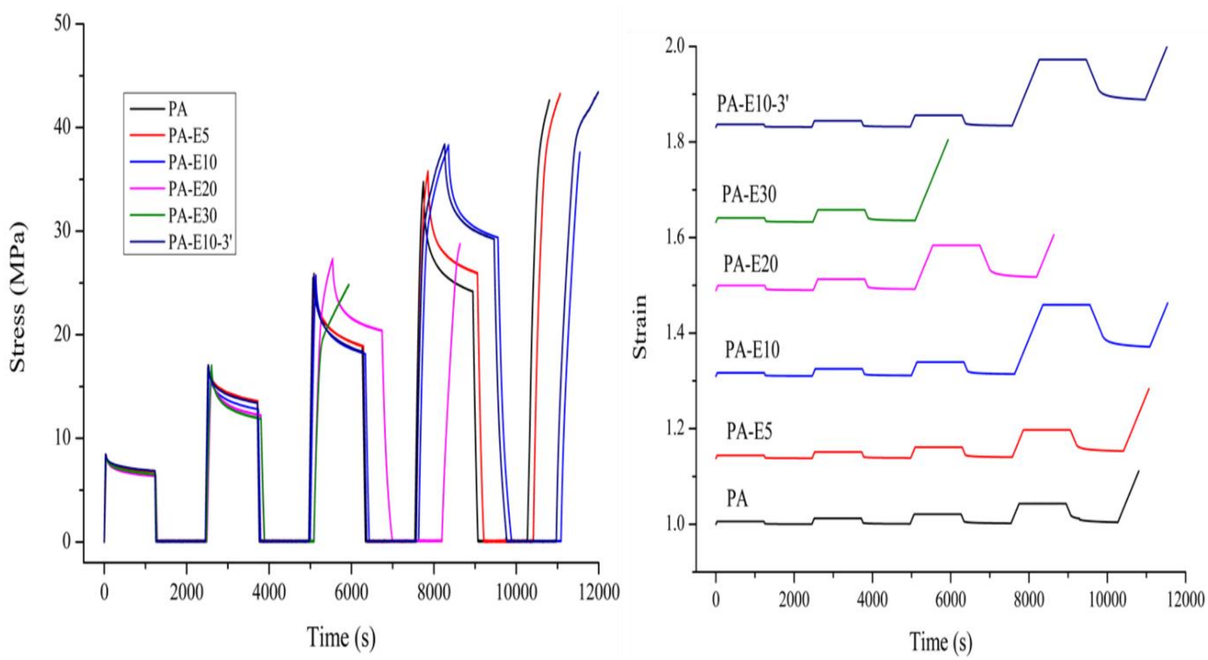

Figure 1. Relaxation response for binary composites

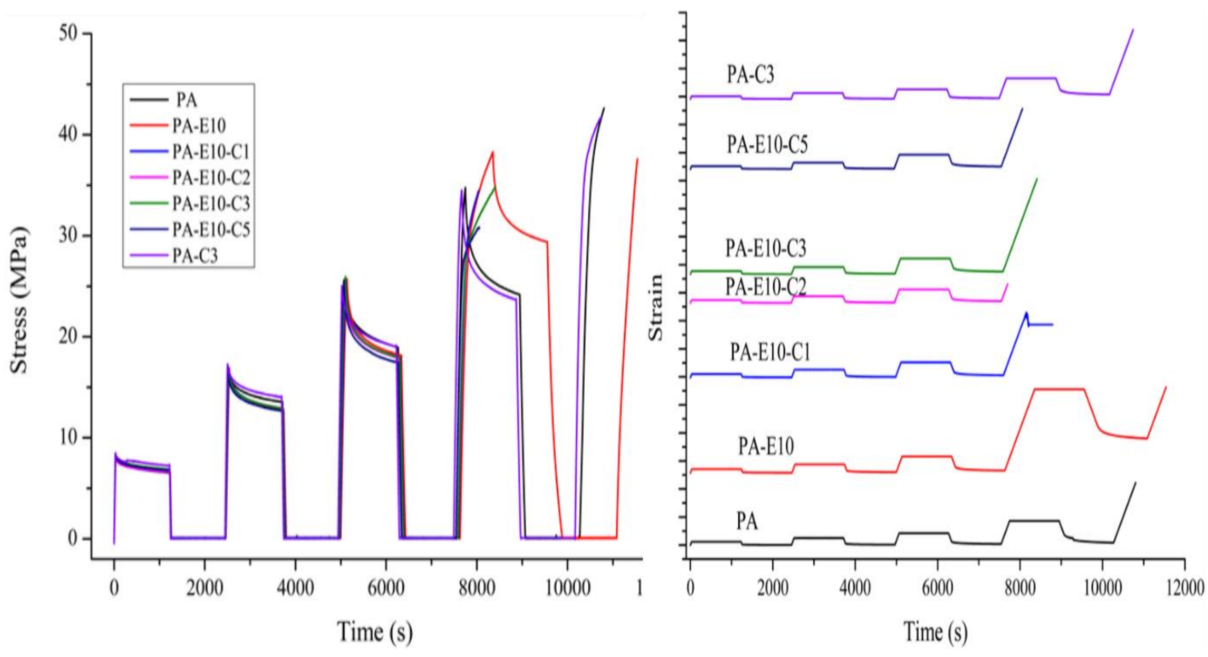

Figure 2. Relaxation response for ternary nanocomposites

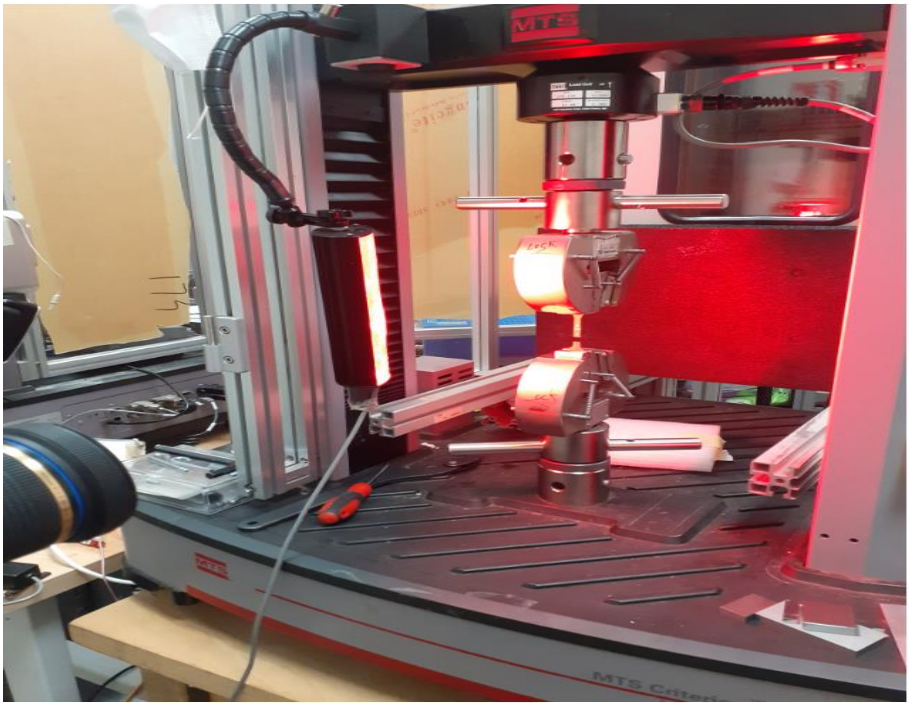

Figure 3. PA12 composite sample specimen between the lower base and upper fixture which had undergone uniaxial cyclic testing.

3.0 Results and Discussions

3.1 Stress relaxation

Stress relaxation is a time-dependent decrease in stress under a constant strain or it is also considered as the change in force as a function of time. Figs. 1 and 2 shows the stress relaxation behaviour of unfilled PA12 with different mixing ratios of EPDM elastomer and nano-clay. For binary composite blends, it was discovered from Fig. 1 that neat PA, PA-E5, PA-E10 and PA-E10-3′ completed four cycles before deformation set in compared to blends with PA-E20 and PA-E30. This means that the later blends displayed lesser elastic responses compared to the former. Furthermore, blend with higher mass fraction of EPDM of 30% exhibited the lowest elastic response compared to neat PA. This may be because of low-frequency response of different blend systems which is controlled by the relaxation mechanisms (Mazidi & Aghjeh, 2015) which is related to interfacial region between the components and the matrix. In a similar way, Fig. 2 shows that ternary nanocomposites with different ratios of clay could not make it to the fourth cycle indicating that the addition of clay into the PA/EPDM reduced the elastic response of the nanoblends. However, the ability to elongate is dependent upon the dispersion and size distribution of EPDM particles (Aritonang et al., 2020). Inorganic particles are rigid and have a much higher stiffness than the thermoplastic matrix. Incorporation of C30B into the PA12/EPDM decreased the strain at break (Wang et al., 2019). Increasing the amounts of C30B contents further decreased the values of strain at break for all the nanocomposite blends. This means that on addition of nano-clay, the strain at break of PA12/EPDM/C30B nanocomposites decreases in comparison with the binary PA12/EPDM blend at lower EPDM content (5 – 10 w.t%). This decrease in strain at break with addition of organoclay is attributed to the decrease in ductility with increased stiffness caused by clay′s uniform dispersion in copolymer matrix. This restricts rubber effect and mobility of the polymer chains in the presence of clay platelets (Baniasadi et al., 2021).

3.2 The cyclic tension

The cyclic loading outcome of the PA12 composites with different mass fraction of EPDM or C30B binary or ternary nanocomposites are shown in Figs. 4 and 5. From the tests, the stress was increased in a separate manner from 10 MPa to 40 MPa. This vividly indicates that an increase in the stress response can be realized with increasing the wt % of either EPDM in the binary composites or C30B in the ternary nanocomposites, meaning that EPDM or C30B can potentially affect the mechanical response (Ghanta et al., 2020; Rostami et al., 2022; Archibong et al., 2023). Mullin’s effect is an aspect of mechanical response in filled rubbers of the stress-strain curve which depends on the maximum loading previously encountered (Srivastava & Mishra, 2018; Fazekas & Goda, 2021; Zhu & Zhong, 2021). This occurs when there is an expansion of the specimen at a constant deformation rate. For instance, from the starting point to the end point of each cycle. In all the composites, a clear Mullins effect can be noticed as the stress in the reloading operation is lesser than the response of the virgin specimens until striking the beginning of maximum applied strain (Clough et al., 2016; Millereau et al., 2018). Also, the C30B remarkably affect the Mullin's effect as reported in (Bokobza, 2023; Yin et al., 2024). A smaller hysteresis loop can be noticed with increase in the amount of C30B into the neat PA blend. Meanwhile, the residual strain after unloading is firmly related with the existence of nano-clay. PA12 composites with mass fraction of EPDM and C30B fillers exhibited similar response.

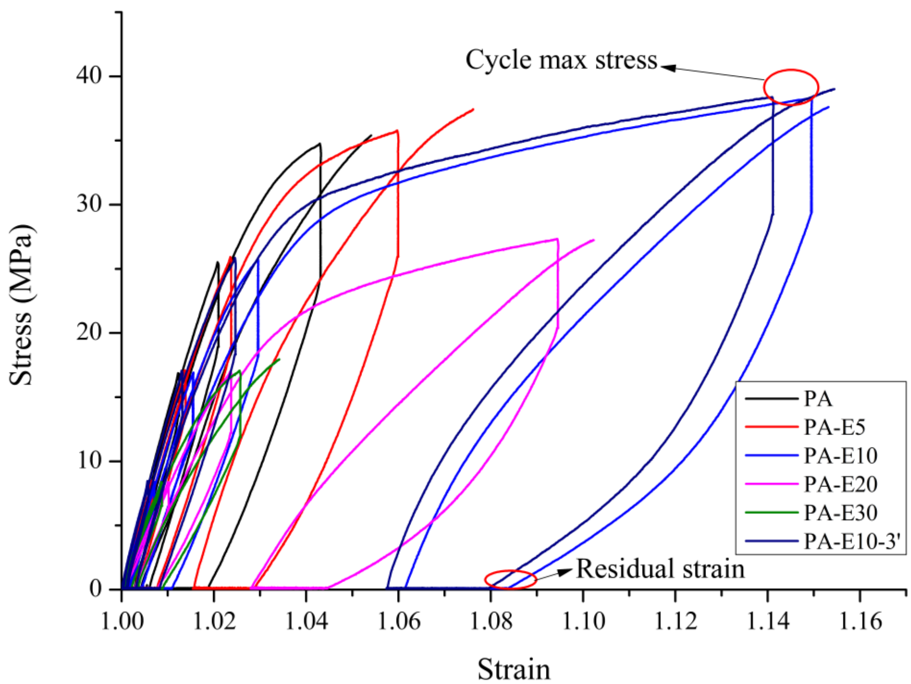

Figure 4. A schematic curve for the area of hysteresis loop, maximum stress, and residual strain for binary composites

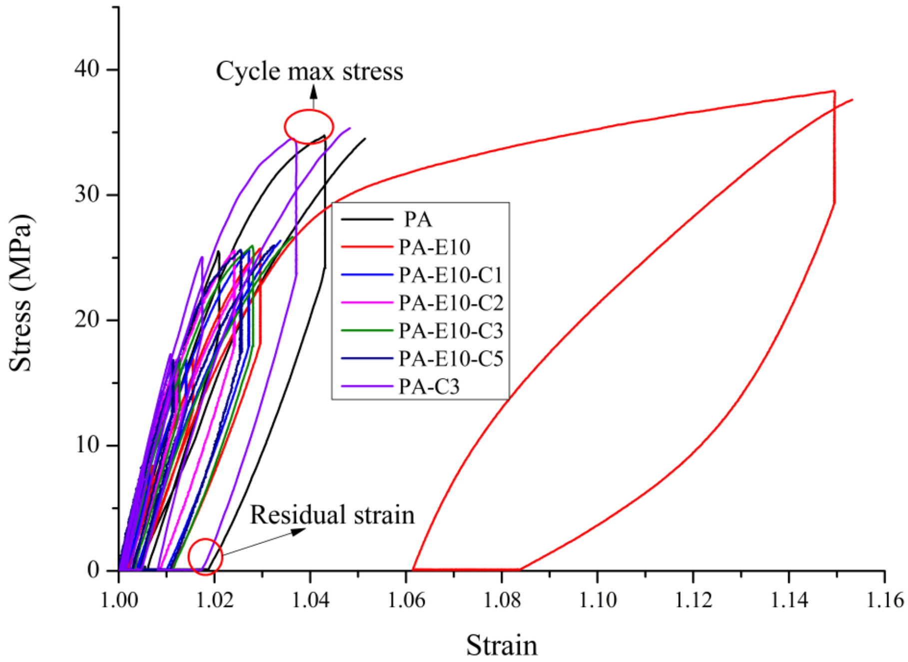

Figure 5. A schematic curve for the area of hysteresis loop, maximum stress and residual strain for binary/ternary nanocomposites

4.0 Conclusion

The hysteresis of PA12/EPDM polymeric blends filled with nano-clay has been evaluated using cyclic test. In this study, we investigated the mechanical performance of elastomer and C30B composites using cyclic tension and stress relaxation. The significance of this research is to recycle waste rubber using thermoplastics. Specifically, we processed a series of PA12 composites with different mass fraction of EPDM. The stress relaxation tests show that the filled PA-E10 and PA-E10-3' displays a viscoelastic relaxation response and EPDM with lower and higher mass fraction greater than 10 shows lesser relaxation. With this, blends with higher mass fraction of EPDM of 30% exhibited the lowest elastic response compared to pure PA. This may be because of low-frequency response of different blend systems which is controlled by the relaxation mechanisms. The stiffness of the filled PA12/EPDM composites increases with increase in C30B mass fraction. Both EPDM and C30B composites exhibits a vivid Mullins effect. The area of hysteresis loop depends on the mass fraction of EPDM and C30B. A smaller hysteresis loop can be noticed with increase in the amount of C30B into the pure PA blend. Meanwhile, the residual strain after unloading is firmly related with the existence of nano-clay. Therefore, cyclic test is a nice tool for determining the Mullins effect of polymeric composites. Further research work should be based on modelling the outcome of the experiment for optimization of our results.

Acknowledgments

The authors are grateful to our respective universities for creating the enabling environment for this work.

References

Aït Hocine, N., Médéric, P., & Hassan, H., 2019. Influence of mixing energy on the solid-state behavior and clay fraction threshold of PA12/C30B® nanocomposites. *Journal of Polymer Engineering*, *39*(6), 565–572. https://doi.org/10.1515/polyeng-2018-0307

Archibong, F. N., Orakwe, L. C., Ogah, O. A., Mbam, S. O., Ajah, S. A., Okechukwu, M. E., Igberi, C. O., Okafor, K. J., Chima, M. O., & Ikelle, I. I., 2023. Emerging progress in montmorillonite rubber / polymer nanocomposites : a review. *Journal of Material Science*, 1–30. https://doi.org/10.1007/s10853-023-08173-4

Aritonang, B., Tamrin, Wirjosentono, B., & Eddiyanto., 2020. Effect of Graft copolymerization of oleic acid on to cyclic natural rubber in polyamide. *Case Studies in Thermal Engineering*, *21*, 100690. https://doi.org/10.1016/j.csite.2020.100690

Avanzini, A., Tomasoni, M., Xu, Z., Berto, F., & Razavi, N., 2024. Fracture assessment of polyamide 12 (PA12) specimens fabricated via Multi Jet FusionTM in the presence of geometrical discontinuities. *Engineering Fracture Mechanics*, *303*, 1–18. https://doi.org/10.1016/j.engfracmech.2024.110118

Banerjee, P., Hazra, A., Ghosh, P., Ganguly, A., Murmu, N. C., & Chatterjee, P. K., 2019. Waste Management and Resource Efficiency. In *Waste Management and Resource Efficiency*. Springer Singapore. https://doi.org/10.1007/978-981-10-7290-1

Baniasadi, H., Trifol, J., Ranta, A., & Seppälä, J., 2021. Exfoliated clay nanocomposites of renewable long-chain aliphatic polyamide through in-situ polymerization. *Composites Part B: Engineering*, *211*(September 2020). https://doi.org/10.1016/j.compositesb.2021.108655

Baran, A., Chatterjee, T., & Naskar, K., 2020. Dynamically vulcanized blends of UHM-EPDM and polypropylene: Role of nano-fillers improving thermal and rheological properties. *Materials Today Communications*, *25*(May), 101486. https://doi.org/10.1016/j.mtcomm.2020.101486

Beerli, T., Roth, C. C., & Mohr, D., 2024. Acta Materialia Semi-automatic miniature specimen testing method to characterize the plasticity and fracture properties of metals. *Acta Materialia*, *263*, 119539. https://doi.org/10.1016/j.actamat.2023.119539

Benneghmouche, Z., & Benachour, D., 2019. Effect of organophilic clay addition on properties of SAN/EPDM blends. *Composite Interfaces*, *26*(8), 711–727. https://doi.org/10.1080/09276440.2018.1531655

Bokobza, L., 2023. Elastomer Nanocomposites : Effect of Filler – Matrix and Filler – Filler Interactions. *Polymers*, *15*(2900), 1–22.

Chafidz, A., Tamzysi, C., Kistriyani, L., Kusumaningtyas, R. D., & Hartanto, D., 2019. Mechanical Properties of PP / Clay Nanocomposites Prepared from Masterbatch : Effect of Nanoclay Loadings and Re-Processing. *Advanced Materials and Application II*, *805*, 59–64. https://doi.org/10.4028/www.scientific.net/KEM.805.59

Clough, J. M., Creton, C., Craig, S. L., & Sijbesma, R. P., 2016. Covalent Bond Scission in the Mullins Effect of a Filled Elastomer: Real-Time Visualization with Mechanoluminescence. *Advanced Functional Materials*, *26*(48), 9063–9074. https://doi.org/10.1002/adfm.201602490

Dorigato, A., Brugnara, M., & Pegoretti, A., 2017. Novel polyamide 12 based nanocomposites for industrial applications. *Journal of Polymer Research*, *24*(96), 1–13. https://doi.org/10.1007/s10965-017-1257-9

Fazekas, B., & Goda, T. J., 2021. Constitutive modelling of rubbers: Mullins effect, residual strain, time-temperature dependence. *International Journal of Mechanical Sciences*, *210*, 1–17. https://doi.org/10.1016/j.ijmecsci.2021.106735

Fazli, A., & Rodrigue, D., 2020. Waste rubber recycling: A review on the evolution and properties of thermoplastic elastomers. *Materials*, *13*(3), 1–31. https://doi.org/10.3390/ma13030782

Ghanta, Tarun Sai, Sridhar Aparna, Namrata Verma, D. P., 2020. Review on nano-and microfiller-based polyamide 6 hybrid composite : Effect on mechanical properties and morphology. *POLYMER ENGINEERING AND SCIENCE*, 1–43. https://doi.org/10.1002/pen.25447

Guan, X., Huang, B., Li, Z., Ma, X., & Liang, B., 2023. Characterizing Tensile Strength of Building Sandstone via Uniaxial Tensile, Compressive, and Flexural Bending Tests. *Materials*, *16*(9), 1–20. https://doi.org/10.3390/ma16093440

Gujre, N., Mitra, S., Soni, A., Agnihotri, R., Rangan, L., Rene, E. R., & Sharma, M. P., 2021. Speciation, contamination, ecological and human health risks assessment of heavy metals in soils dumped with municipal solid wastes. *Chemosphere*, *262*, 128013. https://doi.org/10.1016/j.chemosphere.2020.128013

Hassan, H., Hocine, N. A., Médéric, P., Deffarges, M. P., & Poirot, N., 2015. Thermal and mechanical properties of PA12/C30B nanocomposites in relationship with nanostructure. *Journal of Applied Polymer Science*, *132*(18), 1–10. https://doi.org/10.1002/app.41938

Jeddi, J., Yousefzade, O., Babaei, A., Ghanbar, S., & Rostami, A., 2017. Morphology, microstructure and rheological properties of SAN (styrene-acrylonitrile)/EPDM (ethylene-propylene-diene monomer) nanocomposites: Investigating the role of organoclay type and order of mixing. *Materials Chemistry and Physics*, *187*, 191–202. https://doi.org/10.1016/j.matchemphys.2016.12.001

Khlystov, N., & Zheng, J., 2013. *Uniaxial Tension and Compression Testing of Materials*. 1–19.

Kondo, M. Y., Montagna, L. S., de Melo Morgado, G. F., de Castilho, A. L. G., dos Santos Batista, L. A. P., Botelho, E. C., Costa, M. L., Passador, F. R., Rezende, M. C., & Ribeiro, M. V., 2022. Recent advances in the use of Polyamide-based materials for the automotive industry. *Polimeros*, *32*(2), 1–14. https://doi.org/10.1590/0104-1428.20220042

Krairi, A., & Doghri, I., 2014. A thermodynamically-based constitutive model for thermoplastic polymers coupling viscoelasticity, viscoplasticity and ductile damage. *International Journal of Plasticity*, *60*, 163–181. https://doi.org/10.1016/j.ijplas.2014.04.010

Laing, B., De Keyzer, J., Seveno, D., & Van Bael, A., 2020. Adhesion between ethylene-propylene-diene monomer and thermoplastics in two-component injection molding: Effect of dicumylperoxide as curing agent. *Journal of Applied Polymer Science*, *137*(41), 1–20. https://doi.org/10.1002/app.49233

Li, R., Yuan, S., Zhang, W., Zheng, H., Zhu, W., Li, B., Zhou, M., Law, A. W., & Zhou, K., 2019. 3D Printing of Mixed Matrix Films Based on Metal − Organic Frameworks and Thermoplastic Polyamide 12 by Selective Laser Sintering for Water Applications. *Applied Materials & Interfaces*, *11*, 40564–40574. https://doi.org/10.1021/acsami.9b11840

Li, Y., Shen, A., Zhao, B., & Guo, Y., 2024. The frost resistance performance of basalt fiber-reinforced concrete (BFRC) subjected to fatigue loads coupled with hydrodynamic pressure. *Journal of Materials Research and Technology*, *28*, 4830–4845. https://doi.org/10.1016/j.jmrt.2023.12.188

Li, Z., Wen, F., Hussain, M., Song, Y., & Zheng, Q., 2020. Scaling laws of Mullins effect in nitrile butadiene rubber nanocomposites. *Polymer*, *193*(January), 122350. https://doi.org/10.1016/j.polymer.2020.122350

Linul, E., Marsavina, L., & Stoia, D. I., 2020. Mode I and II fracture toughness investigation of Laser-Sintered Polyamide. *Theoretical and Applied Fracture Mechanics*, *106*(December 2019), 102497. https://doi.org/10.1016/j.tafmec.2020.102497

Long, R., & Hui, C. Y., 2016. Fracture toughness of hydrogels: Measurement and interpretation. *Soft Matter*, *12*(39), 8069–8086. https://doi.org/10.1039/c6sm01694d

Mapossa, A. B., da Silva Júnior, A. H., de Oliveira, C. R. S., & Mhike, W., 2023. Thermal, Morphological and Mechanical Properties of Multifunctional Composites Based on Biodegradable Polymers/Bentonite Clay: A Review. *Polymers*, *15*(16), 1–25. https://doi.org/10.3390/polym15163443

Mehrabi Mazidi, M., & Razavi Aghjeh, M. K., 2015. Effects of blend composition and compatibilization on the melt rheology and phase morphology of binary and ternary PP/PA6/EPDM blends. *Polymer Bulletin*, *72*(8), 1975–2000. https://doi.org/10.1007/s00289-015-1384-6

Meyer, N., Saburow, O., Hohberg, M., Hrymak, A. N., Henning, F., & Kärger, L., 2020. Parameter identification of fiber orientation models based on direct fiber simulation with smoothed particle hydrodynamics. *Journal of Composites Science*, *4*(2), 1–20. https://doi.org/10.3390/jcs4020077

Millereau, P., Ducrot, E., Clough, J. M., Wiseman, M. E., Brown, H. R., Sijbesma, R. P., & Creton, C., 2018. Mechanics of elastomeric molecular composites. *Proceedings of the National Academy of Sciences of the United States of America*, *115*(37), 9110–9115. https://doi.org/10.1073/pnas.1807750115

Mahmoud, M., Huitorel, B., & Fall, A., 2024. Rheology and agglomeration behavior of semi-crystalline polyamide powders for selective laser sintering: A comparative study of PA11 and PA12 formulations. *Powder Technology*, *433*, 1–9. https://doi.org/10.1016/j.powtec.2023.119279

Mohankumar, K., Hariharan, V., & Rao, N. P., 2016. Heavy metal contamination in groundwater around industrial estate vs residential areas in Coimbatore, India. *Journal of Clinical and Diagnostic Research*, *10*(4), BC05–BC07. https://doi.org/10.7860/JCDR/2016/15943.7527

Morovati, V., & Dargazany, R., 2019. Micro-mechanical modeling of the stress softening in double-network hydrogels. *International Journal of Solids and Structures*, *164*, 1–11. https://doi.org/10.1016/j.ijsolstr.2019.01.002

Olongal, M., Raphael, L. R., Raghavan, P., Mohamed Nainar, M. A., & Athiyanathil, S., 2021. Maleic anhydride grafted acrylonitrile butadiene styrene (ABS)/zinc oxide nanocomposite: an anti-microbial material. *Journal of Polymer Research*, *28*(8), 1–13. https://doi.org/10.1007/s10965-021-02632-9

Ortega, F. J., Roman, C., Navarro, F. J., García-morales, M., & Mcnally, T., 2016. Physico-chemistry control of the linear viscoelastic behaviour of bitumen / montmorillonite / MDI ternary composites : Effect of the modi fi cation sequence. *Fuel Processing Technology*, *143*, 195–203. https://doi.org/10.1016/j.fuproc.2015.11.011

Petousis, M., Vidakis, N., Mountakis, N., Papadakis, V., & Tzounis, L., 2022. Three-Dimensional Printed Polyamide 12 (PA12) and Polylactic Acid (PLA) Alumina (Al2O3) Nanocomposites with Significantly Enhanced Tensile, Flexural, and Impact Properties. *Nanomaterials*, *12*(23), 1–24. https://doi.org/10.3390/nano12234292

Plagge, J., & Klueppel, M., 2019. Mullins effect revisited : Relaxation , Recovery and high-strain Damage. *Materials Today Communications*. https://doi.org/10.1016/j.mtcomm.2019.100588

Qi, Y., Caillard, J., & Long, R., 2018. Fracture toughness of soft materials with rate-independent hysteresis. *Journal of the Mechanics and Physics of Solids*, 1–53. https://doi.org/10.1016/j.jmps.2018.05.020

Rostami, A., Vahdati, M., Nowrouzi, M., Karimpour, M., & Babaei, A., 2022. Morphology and physico-mechanical properties of poly (methyl methacrylate)/polystyrene/polypropylene ternary polymer blend and its nanocomposites with organoclay: The effect of nature of organoclay and method of preparation. *Polymers and Polymer Composites*, *30*, 1–10. https://doi.org/10.1177/09673911221107811

Salazar, A., Cano, A. J., & Rodríguez, J., 2022. Mechanical and fatigue behaviour of polyamide 12 processed via injection moulding and selective laser sintering. Analysis based on Kitagawa-Takahashi diagrams. *Engineering Fracture Mechanics*, *275*, 108825. https://doi.org/10.1016/j.engfracmech.2022.108825

Schmid, M., Kleijnen, R., Vetterli, M., & Wegener, K., 2017. Influence of the origin of polyamide 12 powder on the laser sintering process and laser sintered parts. *Applied Sciences (Switzerland)*, *7*(5). https://doi.org/10.3390/app7050462

Schroer, A., & Wheeler, J. M., 2018. Deformation behavior and energy absorption capability of polymer and ceramic-polymer composite microlattices under cyclic loading. *Journal of Material Research*, *10*(25), 1–16. https://doi.org/10.1557/jmr.2017.485

Sivaram, S., 2017. Wallace Hume Carothers and the birth of rational polymer synthesis. *Resonance*, *22*(4), 339–353. https://doi.org/10.1007/s12045-017-0474-1

Srivastava, S. K., & Mishra, Y. K., 2018. Nanocarbon reinforced rubber nanocomposites: Detailed insights about mechanical, dynamical mechanical properties, payne, and mullin effects. *Nanomaterials*, *8*(11), 1–56. https://doi.org/10.3390/nano8110945

Stojšić, J., Raos, P., Milinović, A., & Damjanović, D., 2022. A Study of the Flexural Properties of PA12/Clay Nanocomposites. *Polymers*, *14*(3), 1–14. https://doi.org/10.3390/polym14030434

Wang, W. T., Yu, H. N., Potter, K., & Kim, B. C., 2020. Effect of the characteristics of nylon microparticles on Mode-I interlaminar fracture toughness of carbon-fibre/epoxy composites. *Composites Part A: Applied Science and Manufacturing*, *138*(April), 106073. https://doi.org/10.1016/j.compositesa.2020.106073

Wang, X., Zhu, Q., Dong, B., Wu, H., Liu, C., Shen, C., Turng, L., & Geng, T., 2019. The e ff ects of nanoclay and deformation conditions on the inelastic behavior of thermoplastic polyurethane foams. *Polymer Testing*, *79*, 106043. https://doi.org/10.1016/j.polymertesting.2019.106043

Wang, Z. J., Li, Q. J., Cui, Y. N., Liu, Z. L., Ma, E., Li, J., Sun, J., Zhuang, Z., Dao, M., Shan, Z. W., & Suresh, S., 2015. Cyclic deformation leads to defect healing and strengthening of small-volume metal crystals. *Proceedings of the National Academy of Sciences of the United States of America*, *112*(44), 13502–13507. https://doi.org/10.1073/pnas.1518200112

Xiao, R., Mai, T., Urayama, K., Ping, J., & Qu, S., 2021. Micromechanical modeling of the multi-axial deformation behavior in double network hydrogels. *International Journal of Plasticity*, *137*(May 2020), 102901. https://doi.org/10.1016/j.ijplas.2020.102901

Yin, B. of P. on P. E. and H. L. of, Jiao, X., Wen, H., Li, Y., & Li, M., 2024. Effect of Prestrain on Payne Effect and Hysteresis Loss of Carbon-Black-Filled Rubber Vulcanizates: Measurements and Modeling. *Polymers*, *16*(436), 1–14.

Zhu, P., & Zhong, Z., 2021. Constitutive modelling for the mullins effect with permanent set and induced anisotropy in particle-filled rubbers. *Applied Mathematical Modelling*, *97*, 19–35. https://doi.org/10.1016/j.apm.2021.03.031